Mineralogy and Petrology (2006) 88: 479–497
DOI 10.1007/s00710-006-0123-y

Mineralogy and Petrology
Printed in Austria

Genesis of carbonate aggregates in lamprophyres from the northeastern Transdanubian Central Range, Hungary: Magmatic or hydrothermal origin?

T. Azbej[1,2], **C. Szabó**[1], **R. J. Bodnar**[2], and **G. Dobosi**[3]

[1] Lithosphere Fluid Research Laboratory, Department of Petrology and Geochemistry, Eötvös University, Budapest, Hungary
[2] Fluids Research Laboratory, Department of Geosciences, Virginia Polytechnic Institute and State University, Blacksburg, USA
[3] Institute for Geochemical Research, Hungarian Academy of Sciences, Budapest, Hungary

Received May 18, 2005; revised version accepted January 18, 2006
Published online May 11, 2006;
Editorial handling: B. DeVivo

Summary

Carbonate aggregates in Late Cretaceous lamprophyre dikes of the northeastern Transdanubian Central Range (TCR) in Northwest Hungary have been classified into three genetic groups. Type-I dolomite + calcite ± magnesite aggregates have petrographic and geochemical features similar to ocelli described by other workers. Fluid inclusions in Type-I aggregates homogenize between 77 and 204 °C and are of hydrothermal origin. Type-II aggregates are characterized by a polygonal shape and are mostly dolomite. Based on their shape and primary fluid inclusions which homogenize between 95 and 172 °C, these carbonate aggregates are interpreted to fill vugs produced by the dissolution of olivine phenocrysts. Type-III carbonate aggregates show an irregular to polygonal shape and distinct compositional zonation and contain secondary aqueous fluid inclusions. Homogenization temperatures of fluid inclusions are below 104 °C, and zonation patterns suggest partial recrystallization. These carbonate aggregates are most likely xenoliths and xenocrysts from the wall rocks of the lamprophyre melt conduits.

Introduction

An igneous rock is said to have an ocellar texture if the ''phenocrysts'' (ocelli) consist of aggregates of smaller crystals arranged radially or tangentially around

larger, generally euhedral crystals to produce a rounded eyelike appearance (e.g. *Phillpotts*, 1990). Ocelli of globular, carbonate or felsic silicate aggregates are common features of lamprophyres and some alkali basalts (e.g. *Phillpotts*, 1990; *Rock*, 1991). For decades ocelli in igneous rocks were interpreted to be the products of silicate–carbonate or silicate–silicate liquid immiscibility or, rarely, as amygdales or vesicles filled by late stage minerals (e.g. *Phillpotts* and *Hodgson*, 1968; *Ferguson* and *Currie*, 1971; *Hamilton* et al., 1979; *Cooper*, 1979; *Foley*, 1984; *Nédli* and *M. Tóth*, 2003; *Vichi* et al., 2005). Ocelli are not the only occurrence of carbonate minerals in lamprophyres: carbonates are also found as pseudomorphs after olivine, melilite or other minerals, as intergrowths with talc, garnet, etc., and as late veins (*Rock*, 1991). *Rock* (1991) classifies primary and secondary carbonates based on stable isotopic composition of lamprophyres from locations around the world.

Carbonate and silicate ocelli have been described in Late Cretaceous lamprophyre dikes in the Transdanubian Central Range (TCR) in Northwest Hungary (e.g. *Horváth* et al., 1983; *Szabó* et al., 1993). The ocelli have been interpreted to be the result of liquid immiscibility in volatile-rich mafic melts (*Kubovics* et al., 1990). Based on the stable isotopic composition, *Demény* et al. (1994) showed that the ocelli from TCR lamprophyre dikes represent a transition between primary igneous and sedimentary carbonate. They interpreted the isotopic composition of the aggregates to be the result of hydrothermal fluids, suggesting a genetic model inconsistent with melt immiscibility. Later detailed petrographic, geochemical and fluid inclusion studies of carbonate aggregates (including ocelli) from the TCR lamprophyres (*Azbej*, 2002; *Azbej* et al., 2003) called into question an origin by melt immiscibility or by simple mixing of different fluids. Because the term ''ocelli'' has genetic implications, we will use the more general term 'carbonate aggregates' to describe these features.

The goal of this study is to constrain the genesis of the various types of carbonate aggregates observed in the TCR lamprophyres. Petrographic, cathodoluminescence and electron microprobe analyses of the carbonate aggregates and fluid inclusion microthermometry provide information related to the origin of carbonate aggregates, as well as the late-stage evolution of the TCR lamprophyres.

Geological background and lamprophyre petrology

During the 1980s, unusual alkaline mafic lamprophyre dikes were recognized in quarries in the NE Transdanubian Central Range, Hungary (*Horváth* and *Ódor*, 1984; *Kubovics* et al., 1989), and in several boreholes (*Horváth* et al., 1983; *Szabó*, 1985; *Kubovics* and *Szabó*, 1988; *Kubovics* et al., 1989) (Fig. 1). These rocks are Late Cretaceous in age (*Horváth* et al., 1983; *Embey-Isztin* et al., 1989; *Dunkl*, 1991) and occur as dikes or dike swarms and show consistent petrographic and geochemical features including panidiomorphic granular texture, high color index, ocelli content, high volatile and incompatible element abundances and similar ages (*Szabó* et al., 1993). Clinopyroxene and olivine occur as phenocrysts in the lamprophyres, and many of the olivine grains are altered. The groundmass is characterized by a framework of clinopyroxene and mica microphenocrysts among carbonate, feldspar, apatite and glass. Multiple generations of carbonate-filled veins are also present. Based on modal composition, most of the dike-rocks are

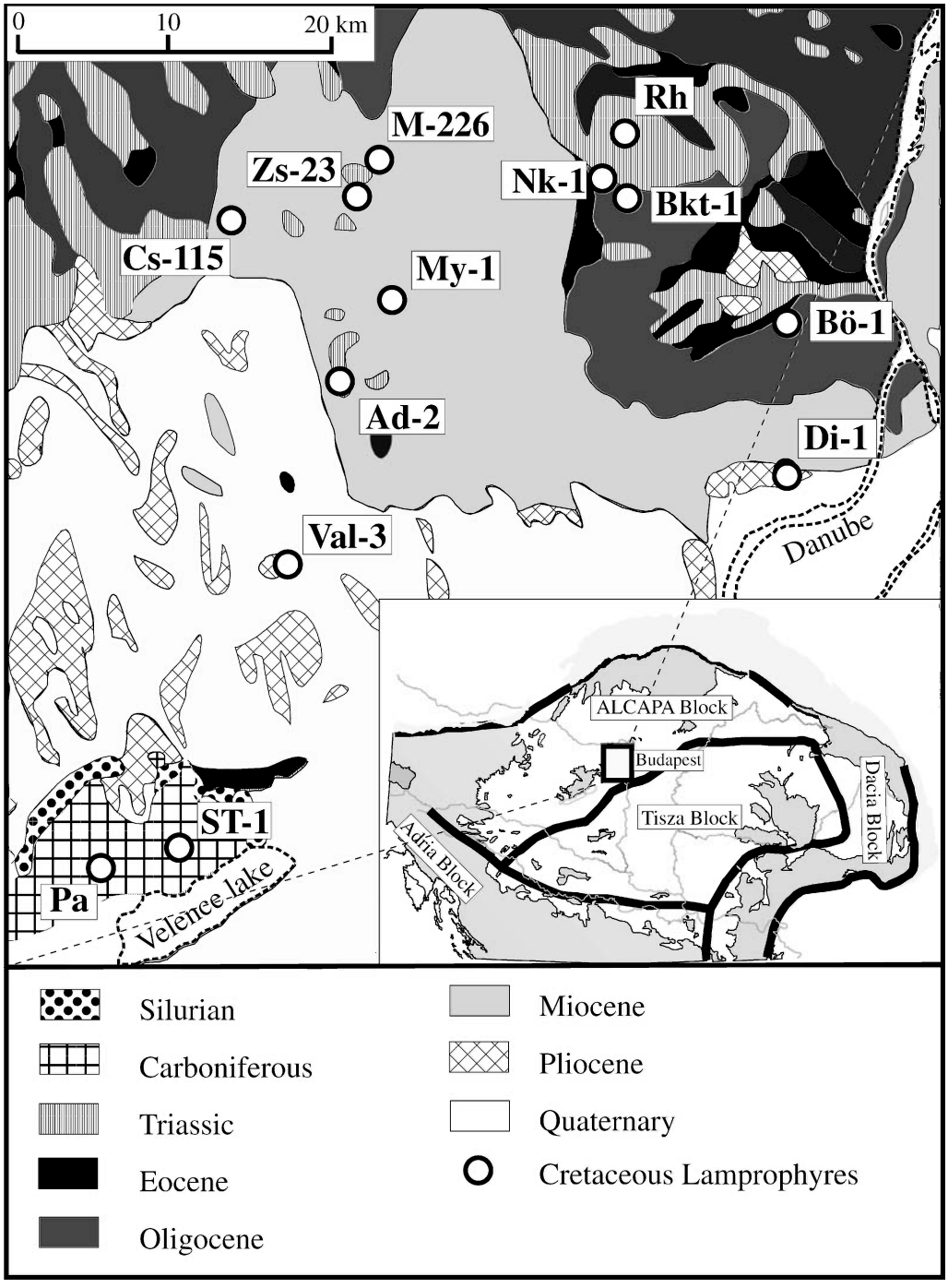

Fig. 1. Geological map of the northeastern Transdanubian Central Range (TCR). Black circles show locations of lamprophyres in outcrop and drill holes (from *Szabó* et al., 1993). Fluid inclusion and chemical data on host phases were obtained from outcrop samples Pá and Rh, and drill core samples Ad-2, Bkt-1, Bö-1, My-1, St-1, Vál-3; inset map shows the Carpathian-Pannonian Region and the study area [black box] (Azbej, 2002)

classified as monchiquite, but camptonite and alnoite also occur (*Embey-Isztin* et al., 1989; *Kubovics* and *Szabó*, 1988; *Kubovics* et al., 1989; *Szabó* et al., 1993). Some dikes contain many upper mantle to crustal xenoliths and xenocrysts (*Szabó*, 1985; *Kubovics* et al., 1985, 1989). The dikes are emplaced into Carboniferous granites, Upper Permian sandstones, Triassic carbonates and andesites. Some carbonatite-like dikes classified as beforsite are found in the St-1 borehole (*Horváth* et al., 1983). The St-1 samples are composed of dolomite (occurring as carbonate aggregates), phlogopite and plagioclase as dominant phases (*Horváth* et al., 1983). Another carbonatite-like dike containing mostly calcite and phlogopite has been described in the Ad-2 borehole (*Szabó* et al., 1993).

Geochemical characteristics suggest that the lamprophyric melt was intruded into an intra-plate extensional tectonic zone (*Kázmér* and *Szabó*, 1989). Accordingly, lamprophyres are typical of Alpine nappe units located at the outer edge of the accretionary wedge. During the Cretaceous these Alpine nappe units were part of a continental basement far away from the inferred Penninic subduction zone (*Kázmér* and *Szabó*, 1989; *Kubovics* et al., 1989). The most likely origin of the parental lamprophyric melt is through a small degree of partial melting of metasomatized lithospheric mantle (*Szabó*, 1985; *Szabó* et al., 1993).

Samples studied and analytical methods

Samples were collected from 11 dikes exposed in 2 surface outcrops (4 representative samples: Pá/1, Pá/2, Rh/121, Rh/1012) and 6 boreholes (nine representative samples: Ad-2/II, Ad-2/III, Ad-2/VIII, Ad-2/X, Bkt-1/6, Bö-1/16, My-1/1, St-1/1 Vál-3/2) (Fig. 1). In addition, data from 6 samples collected by *Demény* et al. (1994) (Ad-2, Bkt-1, Bö-1, Pá, Rh, St-1) have been incorporated into this present study.

Electron microprobe analyses were carried out on a JEOL Superprobe JXA-8600 WDS at the Department of Earth Sciences, University of Florence and on a Cameca SX-50 at the Department of Geosciences at Virginia Tech. The accelerating voltage was 15 kV, with a 10 nA sample current. Mineral analyses were performed using a beam diameter of 10 μm. Counting times were 20 seconds for all elements. Natural mineral standards were employed, and the correction method of *Bence* and *Albee* (1968) was applied at the University of Florence, and the ZAF technique was used at Virginia Tech. Backscattered electron images were collected using a JEOL Superprobe 733, equipped with an INCA Energy 200 EDS, at the Institute for Geochemical Research of the Hungarian Academy of Sciences using an accelerating voltage of 20 kV with a 3 nA sample current.

Microthermometric analyses were carried out on a Linkam THMS 600 stage at Virginia Tech. Cathodoluminescence studies were carried on a Technosyn 8200 MK II cold cathodoluminescence microscope at Virginia Tech using a sample current of 600 nA and an accelerating voltage of 10 kV.

Petrography

Szabó et al. (1993) reported ocelli from the TCR lamprophyres that contained calcite and dolomite, radial and acicular micas, sanidine, analcime, and oxide

minerals, but these authors did not subdivide the ocelli into different types based on textures. In the present study, three textural groups of carbonate aggregates were distinguished. The volume of carbonate aggregates in the lamprophyres varies from about 1 to 45%.

The temporal classification of fluid inclusions in the carbonate aggregates of the TCR lamprophyres was determined based on petrographic characteristics of the inclusions (*Goldstein* and *Reynolds*, 1994; *Bodnar*, 2003a). Inclusions that occur along fractures cross-cutting mineral grains were classified as secondary. Inclusions that appeared to be isolated and not along obvious fractures were interpreted to be primary.

Type-I aggregates have petrographic features characteristic of typical ocelli (Fig. 2A) and show a globular shape and are approximately 0.2 to 4.0 mm in diameter. In addition to carbonate minerals, silicates (nepheline, analcime, sanidine) and rarely chalcedony are present either as anhedral phases occurring in the interior, or as elongated subhedral phases intersecting the rim of the aggregates (Fig. 2B). In some samples phlogopite flakes occur tangentially at the rim of the carbonate aggregates (Fig. 2C). The carbonate minerals contain primary fluid inclusions.

Type-II aggregates are found mostly in samples from the St-1 and rarely Ad-2 dikes. The size varies from 0.2 to 3.5 mm in diameter. Their shapes and sizes are similar to those of olivine phenocrysts in the TCR lamprophyres (Fig. 2D). Type-II aggregates contain minor chalcedony and primary fluid inclusions. Some thin sections reveal multiple generations of carbonate veins intersecting each other and Type-I and Type-II carbonate aggregates, forming a network (Fig. 2G, H).

Type-III aggregates are irregular to polygonal in shape (Fig. 2E, F), and vary between 0.1 and 3.0 mm in diameter. In addition to the dominant carbonate phases, clay minerals sometimes occur near the rim (Fig. 2F). Cathodoluminescence and SEM images reveal chemical zonation in these aggregates (Fig. 2F) in contrast to the relatively homogenous patterns observed in Type-I and Type-II aggregates (*Azbej*, 2002). Type-III carbonate aggregates contain secondary fluid inclusions.

Chemical composition of carbonate aggregates

Several carbonate aggregates in each of seventeen samples from eight sample localities (Fig. 1, Fig. 3A, B; Tables 1, 2) have been analyzed. Type-I aggregates consist of calcite, dolomite and minor magnesite (Table 1) and show no compositional or petrographic zoning or evidence of exsolution. Type-II aggregates are composed of ferroan dolomite with FeO of 0.5 to 9.1 wt% and SrO up to 1.7 wt% (Table 2).

A diagnostic characteristic of Type-III aggregates is their zoned texture (Fig. 2E, F). Based on electron microprobe traverses, a trend from calcite → dolomite → magnesite or from dolomite → magnesite is observed from the core to the rim in several Type-III aggregates. The thickness of individual zones is on the order of 100 µm. Sometimes ankerite is also observed at the rims. Similar compositional zonation has been reported from the Rh sampling locality by *Demény* et al. (1994) where a carbonate aggregate with calcite core and dolomite rim was found.

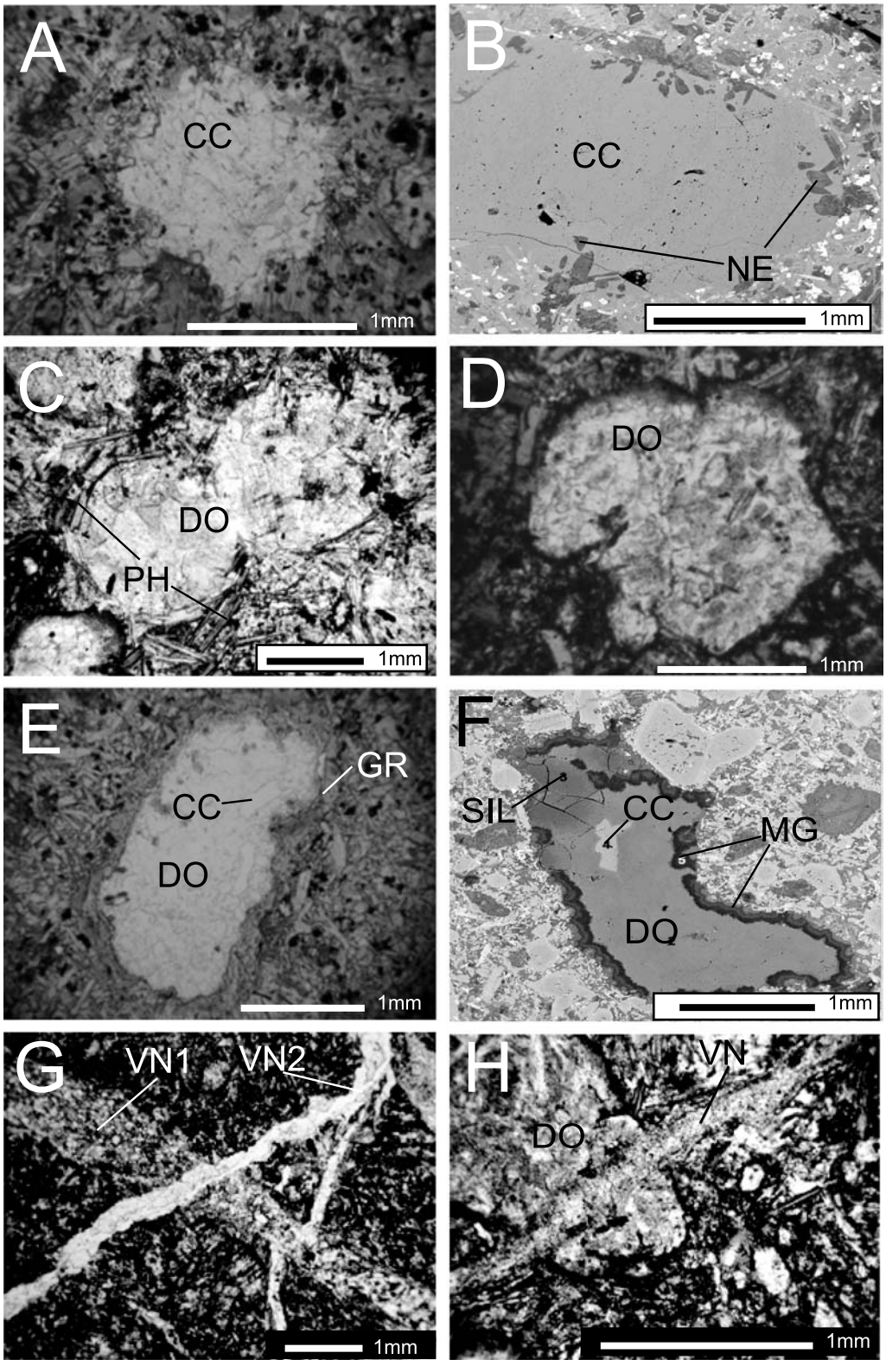
A
CC
1mm
B
CC
NE
1mm
C
DO
PH
1mm
D
DO
1mm
E
GR
CC
DO
1mm
F
SIL
CC
MG
DO
1mm
G
VN1
VN2
1mm
H
VN
DO
1mm

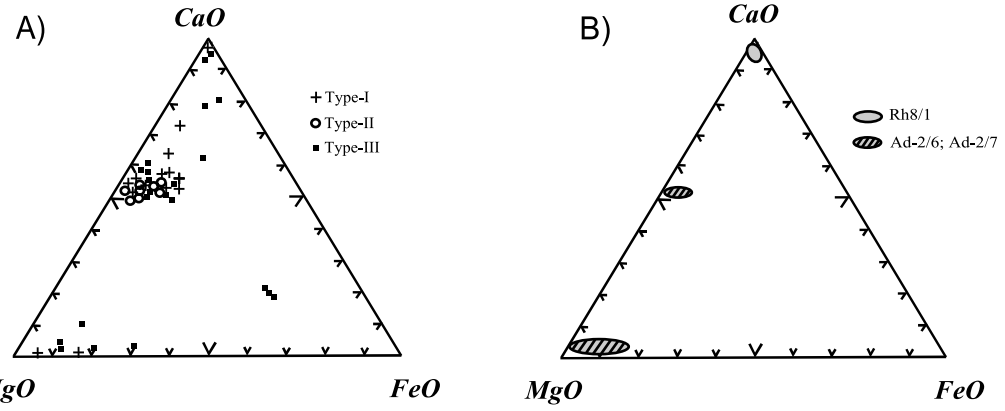

Fig. 3. Ternary CaO–MgO–FeO diagrams showing compositions of carbonate phases in aggregates from the TCR lamprophyres. **A** Type-I, Type-II and Type-III aggregates in samples from outcrops (Pa, Rh) and drill cores (Ad-2, Bkt-1, Bö-1, My-1, St-1, Vál-3). **B** Composition of carbonates in samples Ad-2/6, Ad-2/7 and Rh/8 after *Demény* et al. (1994)

Demény et al. (1994) also mention zoned aggregates containing dolomite and magnesite from lamprophyres in the Ad-2 borehole.

All aggregates have relatively high trace and minor element concentration compared to the composition of the Triassic carbonate wall-rocks presented by *Balog* et al. (1999). Carbonate veins have been analyzed and compared to the composition of carbonates in coexisting aggregates (Table 3). In each of the samples the composition of veins showed similar variation as of the aggregate carbonates. The composition of vein filling carbonates varies from predominantly calcitic (e.g. Ad-2) to ankeritic (Bö-1/16, St-1) (Table 3).

Microthermometric analyses

The formation temperature of carbonate aggregates in the TCR lamprophyres was estimated based on microthermometric analyses of fluid inclusions and chemical compositions of coexisting silicate phases in predominantly carbonate aggregates.

Fig. 2. Photomicrographs (A, C, D, E, G, H) and BSE images (B, F) of carbonate aggregates in the TCR lamprophyres. **A** Type-I aggregate containing calcite (CC) in sample St-1/1 (plane-polarized light). **B** Type-I silicate-bearing aggregate containing calcite (CC) and nepheline (NE) in sample My-1/1. **C** Type-I aggregate containing dolomite (DO) surrounded by tangentially aligned phlogopites (PH) in sample St-1/1 (plane-polarized light). **D** Type-II aggregate containing dolomite (DO) in sample St-1/1 (plane-polarized light). **E** Type-III aggregate containing calcite (CC) and dolomite (DO) with glassy rim (GR) in sample Bö-1/16 (plane-polarized light). **F** Mineralogically zoned Type-III aggregate containing calcite (CC), dolomite (DO), magnesite (MG) and Al-silicate (SIL) in sample Rh/1012. **G** Two generations of cross-cutting carbonate veins (VN1, VN2) in sample Ad2-II. **H** Carbonate vein (VN) cross cutting a Type-II dolomite aggregate (DO) in sample St-1

Table 1. *Average composition of carbonate minerals in Type-I aggregates from the TCR lamprophyres*

Aggregate type	Type-I												
Sample	Ad-2/III/3		Bkt1/6	My-1/1		My-1/4		Pá1/1	Pá1/2		St-1/1	St-1/2	Vál3/2
Carbonate phase	Dolomite	Magnesite	Calcite	Calcite	Dolomite	Mg-Calcite	Calcite	Calcite	Calcite	Fe-Dolomite	Dolomite	Dolomite	Dolomite
CaO	29.4	0.11	54.8	55.4	34.4	40.0	55.0	54.2	55.0	31.9	28.7	29.6	28.8
MgO	21.2	46.0	0.12	0.05	13.5	9.99	0.56	0.14	0.21	15.7	18.8	18.9	20.3
FeO	0.49	3.13	0.15	0.12	3.92	3.34	b.d.	0.10	0.19	6.01	4.04	4.06	1.14
MnO	0.13	0.16	b.d.	0.02	0.15	0.35	b.d.	0.16	0.11	0.61	0.31	0.19	0.61
SrO	0.11*	b.d.	0.36	0.35	0.47	0.73	0.45	0.24	0.75	0.20	1.01	0.24	2.05
BaO	0.10*	0.12*	0.09*	0.10	b.d.	b.d.	b.d.	0.13*	0.09*	0.10	0.09*	b.d.	0.10*
Total	51.2	49.4	55.4	56.0	52.5	54.4	56.0	54.8	56.2	54.5	52.8	53.0	52.9
Calc. CO_2	46.6	49.6	43.3	43.7	44.5	44.9	44.0	42.9	43.9	46.3	46.1	46.6	46.7
Calc. Total	98.0	99.0	98.7	99.7	97.0	99.3	100.0	97.8	100.1	100.8	98.9	99.5	99.6
$CaCO_3$ mol%	54.1	0.31	99.0	99.0	63.7	72.1	98.1	98.8	97.9	56.7	52.1	53.4	52.0
$MgCO_3$ mol%	44.7	89.3	0.13	0.12	28.7	20.7	1.13	0.29	0.43	32.1	39.2	39.2	42.0
$FeCO_3$ mol%	0.83	10.1	0.07	0.21	6.65	5.52	0.03	0.17	0.31	9.81	6.69	6.73	1.89
$MnCO_3$ mol%	0.21	0.25	–	0.03	0.26	0.58	–	0.26	0.19	1.00	0.52	0.32	1.02
# of measurements	7	2	3	4	1	1	2	5	3	4	7	3	3

*Highest concentration measured (not average) for a given trace element in the sample
b.d. Below detection limit
Calc. CO_2 Calculated CO_2 wt%
Calc. Total Total wt% oxides (including CO_2)

Table 2. *Average composition of carbonate minerals in Type-II and -III aggregates from the TCR lamprophyres*

Aggregate type	Type-II			Type-III								
Sample	Ad-2/X	St-1/3	St-1/4	Ad-2/IIb	Bö1-16/1		Bö1-16/2		Bö1-16/3	Rh1012/1		Rh1012/3
Carbonate phase	Dolomite	Dolomite	Fe-Dolomite	Dolomite	Calcite	Dolomite	Mg-Calcite	Fe-Dolomite	Ankerite	Calcite	Fe-Dolomite	Magnesite
Aggregate zone	Not zoned	Not zoned	Not zoned	core	core	rim	core	rim	rim	core	rim	rim
CaO	28.8	29.4	29.6	30.7	54.7	11.2	43.9	28.9	1.34	53.2	31.8	1.22
MgO	18.9	17.2	17.4	18.6	0.19	12.0	4.19	16.5	32.8	1.15	18.0	40.7
FeO	5.04	5.78	6.34	3.99	0.11	33.9	6.65	6.69	18.0	0.98	2.54	7.10
MnO	0.17	0.16	0.20	0.09	0.09*	0.63	0.38	0.16	b.d.	0.53	0.47	0.18
SrO	0.29	0.08*	0.10*	0.15	0.95	0.14	0.35	0.10	b.d.	b.d.	0.12*	0.09*
BaO	b.d.	0.09*	b.d.	0.08*	b.d.	b.d.	0.10	b.d.	b.d.	b.d.	0.09*	b.d.
Total	53.3	52.6	53.6	53.5	55.9	57.9	55.6	52.3	52.1	55.8	52.7	49.2
Calc. CO_2	46.6	45.6	46.3	47.0	43.6	43.1	43.4	45.0	47.9	43.9	46.4	49.9
Calc. Total	99.9	98.3	99.9	100.5	99.6	101.0	99.0	97.3	100.0	99.8	99.3	99.2
$CaCO_3$ mol%	51.7	53.7	53.3	55.0	98.0	19.8	81.0	53.4	2.62	95.1	57.5	2.24
$MgCO_3$ mol%	39.0	36.2	35.9	38.1	0.40	24.3	6.90	34.8	68.8	2.36	37.3	85.5
$FeCO_3$ mol%	8.66	9.67	10.4	6.51	0.18	54.7	11.5	11.4	28.6	1.61	4.21	11.9
$MnCO_3$ mol%	0.27	0.27	0.33	0.14	0.14	0.97	0.63	0.25	–	0.87	0.78	0.29
# of measurements	2	9	5	4	4	3	2	6	1	3	3	4

*Highest concentration measured (not average) for a given trace element in the sample
b.d. Below detection limit
Calc. CO_2 Calculated CO_2 wt%
Calc. Total Total wt% oxides (including CO_2)

Table 3. *Average composition of carbonate minerals in veins from the TCR lamprophyres*

Sample Carbonate phase	Ad-2/II Calcite	Bö-1-16 Ankerite	St-1/5 Fe-Dolomite
CaO	54.2	3.07	28.5
MgO	0.71	32.3	9.83
FeO	1.51	16.4	16.7
MnO	0.18	0.24	0.11
SrO	0.12*	0.13*	0.12
BaO	0.10*	0.10*	b.d.
Total	56.5	52.0	55.2
Calc. CO_2	42.8	47.7	43.3
Calc. Total	99.3	99.8	98.5
$CaCO_3$ mol%	95.9	5.04	51.5
$MgCO_3$ mol%	1.74	73.6	24.7
$FeCO_3$ mol%	2.09	21.0	23.6
$MnCO_3$ mol%	0.25	0.31	0.15
# of measurements	3	7	2

*Highest concentration measured (not average) for a given trace element in the sample
b.d. Below detection limit
Calc. CO_2 Calculated CO_2 wt%
Calc. Total Total wt% oxides (including CO_2)

According to *Boettcher* et al. (1980), the water-saturated solidus of magmatic carbonate is above 565 °C at pressures less than 5 kbars. Thus, carbonates of hydrothermal origin would be expected to precipitate below 565 °C.

Primary fluid inclusions in Types-I and -II aggregates and secondary inclusions in Type-III carbonates were analyzed. The carbonate veins did not contain fluid inclusions suitable for microthermometric analysis. Fluid inclusions in Types-I and -II aggregates are scattered randomly in the host mineral, and show no alignment along fracture planes or growth zones. These inclusions are interpreted to be of primary origin based on mode of occurrence. The inclusions vary from $<2\,\mu m$ to about 14 μm, contain vapor and liquid at room temperature and have irregular to regular negative-crystal shape.

Type-III aggregates contain secondary fluid inclusions along roughly planar, sometimes branching, healed fractures that do not extend to the rim of the aggregates. The inclusions are $<4\,\mu m$, contain liquid and vapor at room temperature, and have an irregular shape. The Type-III aggregates also contain a few randomly distributed inclusions which would be classified as primary based on their occurrence. However, the homogenization temperature and salinity of these inclusions is similar to that of the obviously secondary inclusions. We interpret these randomly distributed inclusions to be either secondary inclusions or primary inclusions that have reequilibrated and/or refilled. This interpretation is based on the assumption that any primary inclusions in the carbonate that were trapped when it was originally precipitated at depth would have reequilibrated when they were entrained into the hot lamprophyric magma during transport to the near-surface (*Bodnar*, 2003b).

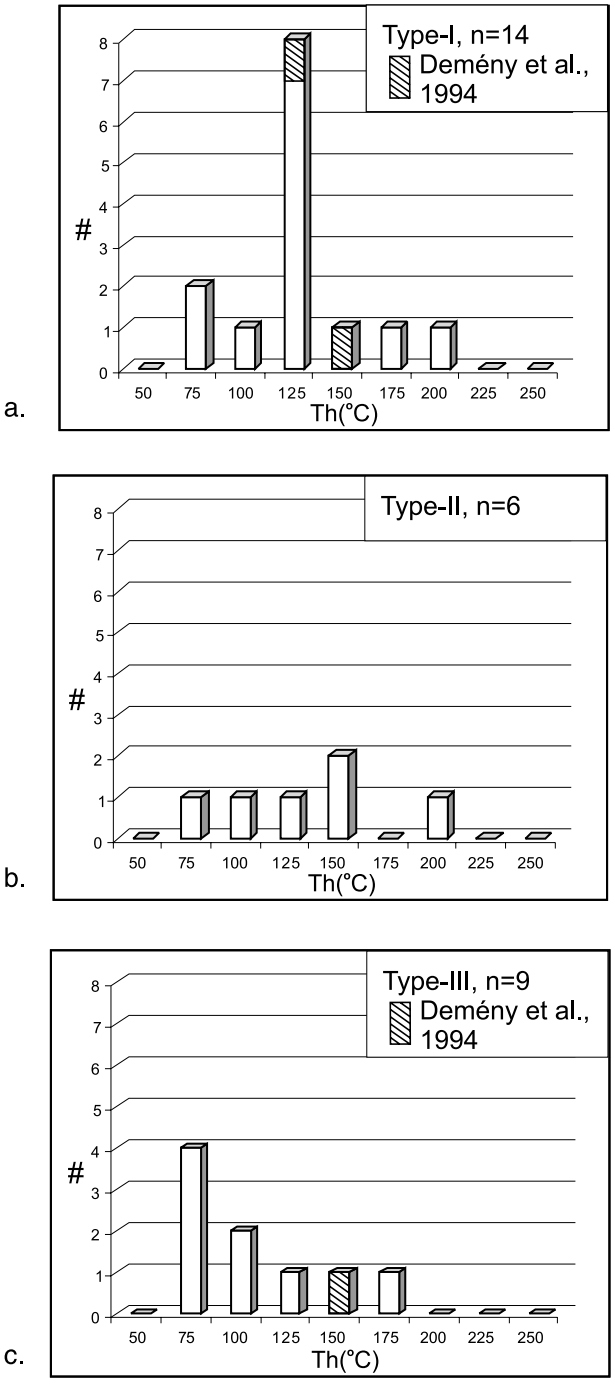

Fig. 4. Homogenization temperatures of fluid inclusions hosted in carbonate aggregates in TCR lamprophyres sorted according to the aggregate type. Data for Type-I and Type-III aggregates include results from *Demény* et al. (1994)

Homogenization temperatures range from 77 to 204 °C (Fig. 4a, c) and are consistent with data reported by *Demény* et al. (1994) on primary fluid inclusions in carbonate ocelli from some TCR lamprophyre dikes. However, our data show a wider temperature range (Fig. 4a). Fluid inclusions in Types-I and -II carbonates span the entire temperature range mentioned above (Fig. 4a, b)

Table 4. *Average ice-melting temperatures and salinities of fluid inclusions in carbonate aggregates from the TCR lamprophyres*

Aggregate type	Sample	Average Th (°C)	S.D.	Average Tm (°C)	Salinity ($NaCl_{equiv.}$ wt%)	S.D.
Type-I	St-1/4a	141	2.2	−9.6	13.6	n/a
	St-1/4b	n/a	n/a	−7.3	10.9	n/a
	My-1/1	204	4.3	−3.3	5.4	1.5
	Pá-1/1	102	33.1	n/a	n/a	n/a
	Bkt1/6	130	49.3	−0.2	0.3	n/a
Type-II	St-1/1c	111	22.6	−1.0	1.7	2.6
	St-1/3	128	29.7	−1.0	1.7	4.1
Type-III	St-1/6	106	15.1	n/a	n/a	n/a
	My-1/2	158	36.1	−2.43	4.1	2.6
	Rh-121/3	90	6.9	−0.2	0.3	n/a

Th Homogenization temperature
S.D. Standard deviation of measurements
Tm Final melting temperature of ice

whereas fluid inclusions in Type-III carbonates vary within a narrower range (Fig. 4c).

First melting occurs at about −21 °C, near the H_2O–NaCl eutectic temperature (−21.2 °C; *Bodnar*, 1992). No evidence of gases was observed. Final ice melting temperatures in the three aggregate types overlap and vary between −0.2 °C and −15.0 °C, with most between −2.4 °C and −9.6 °C (Table 4). Based on the observed first melting temperatures the inclusions are modeled using the H_2O–NaCl system. Salinities of primary fluid inclusions in Types-I and -II aggregates range from 4.0 to 13.6 $NaCl_{equiv.}$ wt% (*Bodnar*, 1992), ignoring the extreme data (Table 2). Final melting temperatures of secondary inclusions in Type-III aggregates average −1.8 °C, corresponding to an average salinity of 2.8 $NaCl_{equiv.}$ wt%.

Discussion

Geothermometry

The formation temperature of carbonates was estimated using the method of *Hamilton* (1961) for nepheline in equilibrium with carbonates. This method is based on experimentally determined limits of $NaAlSiO_4$–$KalSiO_4$–SiO_2–H_2O solid-solution in nepheline at temperatures between 500 and 775 °C, using the K/Na and Si/Al cation ratios of nepheline in equilibrium with silicate melt (*Hamilton* and *MacKenzie*, 1960). Experiments at 1 and 2 kbars show that the effect of pressure on the solid-solution boundary is negligible (*Hamilton*, 1961). This method was applied to the Type-I aggregates that show textural evidence of coeval crystallization of nepheline and carbonate (Fig. 2B). Two analyzed nephelines contain 73.8 and 82.4 mole% nepheline end-member ($NaAlSiO_4$), 26.2 and 17.6 mole% kalsilite ($KalSiO_4$), and 1.9 and 3.5 mole% SiO_2, respectively, and

Table 5. *Summary of petrographic, geochemical and microthermometric characteristics of different carbonate aggregate types in the TCR lamprophyres*

Aggregate Type	Petrography	Microthermometry	Carbonate Composition	Proposed Origin	Samples
Type-I	Globular shape, Tangentially oriented mica and amphibole at rim	Primary FIs Th between 77 and 204 °C	Dolomite, calcite, magnesite	Hydrothermal filling of vesicles or recrystallization of ocelli	Ad-2/III, Bkt1/6, My-1, Pá1, St-1, Vál-3
Type-II	Polygonal shape, Olivine pseudomorphs, no mica or amphibole rim	Primary FIs Th between 95 and 172 °C	Dolomite	Pseudomorphs after olivine	Ad-2/X, St-1
Type-III	Irregular shape, no mica or amphibole rim, Al-silicates at rim	Secondary FIs Th $\leq$ 104 °C	Compositional zonation: calcite, dolomite, magnesite, $\pm$ ankerite	Carbonate xenoliths and xenocrysts	Ad-2/II, Bö1-16, Rh/1012, Rh8, Bkt1/6

Fls Fluid inclusions

suggest a temperature of formation <500 °C. This temperature is assumed to also apply to the contemporaneous carbonate in the aggregates.

Genesis of the carbonate aggregates

The genesis of Types-II and -III carbonate aggregates can be readily established on the basis of the evidence presented here (Table 5). Petrographic and geochemical characteristics of Type-III carbonates support their xenolithic – xenocrystic origin. Their polygonal, irregular shape (Fig. 2E, F) is consistent with their origin as fragments from the conduits of the intruding lamprophyre melt. The other distinctive geochemical feature of the Type-III aggregates is that they contain Mg- and Fe-rich carbonate phases at the rims, and Ca-rich carbonate cores (Fig. 2E, F).

The geological setting and petrographic and geochemical features of zoned silicate phases (clinopyroxenes, mica) from lamprophyres indicate an extremely rapid cooling rate for the dike rocks (*Szabó* et al., 1993). According to *Fisler* and *Cygan* (1999), distinct carbonate compositional zoning on a scale of 100's of micrometers, such as observed in Type-III carbonate aggregates, is unlikely to be reset by chemical diffusion during rapid cooling (1000 °C/m.y.) of melts in contact with carbonates. Thus, we can exclude chemical diffusion for the origin of compositional zoning observed in Type-III aggregates (Fig. 2E, F). The compositional zonation in Type-III aggregates (Fig. 2E, F; Table 5) is best explained by reaction between the solid carbonate wall rock and hot lamprophyre melt, resulting in rapid melting and crystallization of the rims of carbonate xenoliths.

The preceding interpretation is consistent with phase equilibria in lamprophyre melts, which have liquidus temperatures ≈1200 °C at lower crustal conditions (*Nemec*, 1977; *Esperanca* and *Holloway*, 1987). Most lamprophyre melts are almost completely crystallized after cooling to 250 to 450 °C below the liquidus temperature (*Nemec*, 1977; *Montel* and *Weisbrod*, 1986). Thus, melts interacting with carbonate (limestone and/or dolomite) wallrocks in the upper crust must have been at least 750 °C. Following entrainment of wall-rock fragments, lamprophyric melts rise quickly towards the surface (*Rock*, 1991; *Szabó* et al., 1993) and cool rapidly, leaving little time for complete assimilation of the larger carbonate aggregates. Thus, only the rims of Type-III aggregates show evidence of interaction with the host melts.

The occurrence of Al-silicates such as those observed at the contact between some Type-III carbonate aggregates and the lamprophyre groundmass (Fig. 2F) have been interpreted as the product of partial assimilation of limestone by alkaline and mafic magmas (e.g. *Joesten*, 1977; *Baker* and *Black*, 1980; *Joesten* et al., 1994; *Owens*, 2000). The secondary fluid inclusions are likely to represent hydrothermal fluids related to the late-stage crystallization of the lamprophyre, or to fluids infiltrating the dikes after their complete crystallization.

The shape and size of Type-II carbonate is similar to that of unaltered or partially altered olivine phenocrysts in the lamprophyres (Fig. 2D) and appear to be metasomatic carbonatization products after olivine phenocrysts. This is consistent with observations of *Rock* (1991) who described widespread late-stage or subsolidus autometasomatic alteration of primary minerals in lamprophyres due to their high volatile content. However, primary fluid inclusions in Type-II aggre-

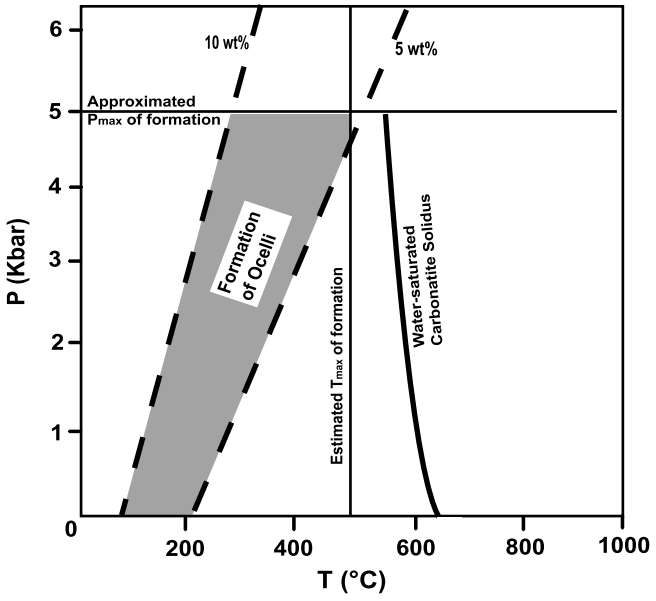

Fig. 5. Estimates of P–T formation conditions for carbonate aggregates in the TCR lamprophyres. The shaded field shows the pressure–temperature field for formation of Type-I carbonate aggregates, defined by the isochores (dashed lines) for lowest and highest measured homogenization temperatures and lowest and highest calculated salinity. The vertical solid line shows the estimated maximum temperature of formation and the horizontal line shows the assumed maximum pressure of formation. Also shown the water-saturated carbonatite solidus from *Boettcher* et al. (1980)

gates are at variance with the proposed gradual carbonatization of olivine. The olivine must have been completely altered and removed to provide space for precipitation of later carbonate phases by hydrothermal fluids, some of which were trapped to produce primary fluid inclusions.

Based on the tectonic and stratigraphic settings of the lamprophyre dike swarms, late stage, secondary process associated with formation of Type-II carbonate aggregates occurred in the upper crust (*Kubovics* and *Szabó*, 1988). Thus, the carbonate aggregates are likely to have formed at pressures lower than 5 kbars. Based on the isochores for aqueous (H_2O–NaCl) fluid inclusions with salinities between 5 and 10 wt% and homogenization temperatures below 200 °C (Fig. 5, Table 4), the formation temperature of these fluid inclusions would have been under 500 °C if the pressure was lower than 5 kbars (Fig. 5). A notable feature is that Type-II aggregates occur exclusively in the St-1 and Ad-2 lamprophyre sample where the abundance of Type-I aggregates with a similar composition is high (Tables 1, 2), as well. This suggests that the source of fluids responsible for the genesis of Types-I and -II carbonates might be the same. This is supported by their similar composition (Fig. 3, Tables 1, 2) and by the fact that there is a network of carbonate veins connecting Types-I and -II aggregates (Fig. 2G, H).

Petrographic and geochemical features of Type-I aggregates are similar to those of aggregates that have been interpreted to be ocelli (e.g. *Phillpotts* and *Hodgson*, 1968; *Ferguson* and *Currie*, 1971). However, most of these authors explained the

genesis of globular aggregates in alkali mafic rocks as solidified droplets of carbonate melt that separated from a silicate melt. Formation of the carbonate phases in the ocelli of TCR lamprophyres, however, cannot be explained by immiscibility during crystallization of the felsic melt. However, the vugs that now contain carbonate could have been formed during such a process.

Primary fluid inclusions in Types I- and -II aggregates show homogenization temperatures lower then 204 °C (Fig. 4). Assuming a formation pressure of <5 kbars for the lamprophyres, the formation temperature of the primary inclusions would have been lower than the water-saturated carbonate solidus (Fig. 5). This conclusion is also supported by the estimated temperature range (lower than 500 °C) for the formation of silicate phases in the ocelli rims that show textural evidence for coeval crystallization with the carbonate phases (Fig. 2B). Most likely Type-I ocelli formed by the following process. First, gas bubbles exsolved from the volatile-rich, late stage melts to produce vesicles in the magma after much of the groundmass had crystallized (*Foley*, 1984; *Andronikov* and *Foley*, 2001). The commonly occurring tangential alignment of phlogopites around aggregates (Fig. 2C) was caused by expansion of gas bubbles in a partially crystallized magma (*Phillips*, 1973). External fluids responsible for the precipitation of Type-I carbonate aggregates were transported through the fracture system now preserved as carbonate-filled veins. The important role of externally derived fluids in the formation of the aggregates is also supported by the mixed magmatic-meteoric isotopic composition of the carbonate aggregates reported by *Demeny* et al. (1994).

Based on the petrographic and geochemical characteristics of Type-I carbonates, one cannot exclude the possibility that they represent recrystallized magmatic carbonates. This also implies that the fluid inclusions do not provide information on the formation of the carbonate aggregates, but rather that the inclusions represent fluids that were present during recrystallization. Among the most diagnostic tests recrystallization has occurred is the presence of geochemical patterns that overprint original compositional zoning (*Goldstein*, 2003). CL and BSE imaging show homogenous cathodoluminescence textures in Type I aggregates. Such textures are usually not associated with recrystallization, but cannot be used to conclusively rule out that recrystallization has occurred.

Results of integrated petrographic, geochemical and fluid inclusion studies suggest that ocelli previously interpreted as products of carbonate–silicate melt immiscibility might be better interpreted as the products of hydrothermal processes.

Conclusions

Late Cretaceous lamprophyres from the Transdanubian Central Range (Hungary) contain carbonate aggregates that have been classified into three distinct groups (Table 5). *Type-I aggregates* are of globular shape, contain primary aqueous fluid inclusions, lack major element zonation, and show tangentially aligned mica at the contact with the host rock. Based on microthermometric analyses and geothermometric calculations, these aggregates precipitated from aqueous hydrothermal solutions to fill vesicles in the crystallized (or partially crystallized) melt. This observation is inconsistent with previous models that explain the genesis of such features by silicate–carbonate melt immiscibility.

Type-II carbonate aggregates also host primary fluid inclusions but show polygonal shape and lack oriented sheet silicates at their rims. Type-II aggregates formed from hydrothermal fluids, similar to those forming Type-I aggregates, except that the carbonate phases precipitated in spaces previously occupied by olivine phenocrysts.

Type-III aggregates have irregular shape, distinct compositional zoning (increasing Mg-, and Fe-content in the carbonate phases towards the rims), contain secondary fluid inclusions, and contain Al-silicates (clay minerals) at the contact with the lamprophyre host, instead of a shell of oriented mica as in Type-I. These aggregates show signs of reaction with the hot lamprophyric melt and are interpreted to represent xenoliths and xenocrysts from the wall rock of the magma conduits.

Acknowledgements

This manuscript has benefited greatly from help of Enikő Bali, Kálmán Török and others at the Lithosphere Fluid Research Laboratory at Eötvös University, Budapest and the Fluids Research Laboratory at Virginia Tech. A. H. Rankin and F. Wall are thanked for their critical comments on an earlier version of this manuscript. Editorial comments of Benedetto De Vivo are also appreciated.

Financial support for this work was provided by TET Hungarian-American Foundation to Csaba Szabó and Robert J Bodnar (17/MO/01) and by Pro Renovanda Culturae Hungariae Foundation to Tristan Azbej and by a grant from the U.S. National Science Foundation to Robert J Bodnar (NSF Grant EAR-0125918).

This is the No. 24 publication of the Lithosphere Fluid Research Lab of the Department of Petrology and Geochemistry at Eötvös University, Budapest.

References

Andronikov AV, Foley SF (2001) Trace element and Nd–Sr isotopic composition of ultramafic lamprophyres from the East Antarctic Beaver Lake area. Chem Geol 175: 291–305

Azbej T (2002) Petrographic and geochemical study on carbonates in lamprophyres (in Hungarian). M.Sc. Thesis. Lithosphere Fluid Research Lab, Eötvös University, Budapest, p 102

Azbej T, Szabó C, Bodnar RJ, Dobosi G (2003) A new interpretation of the genesis of carbonate aggregates from lamprophyres in Hungary: Are ocelli of magmatic or hydrothermal origin? Acta Mineral Petrogr Abst. Ser, Szeged, Abstract Series 2: 12

Baker CK, Black PM (1980) Assimilation and metamorphism at a basalt-limestone contact, Tokatoka, New Zealand. Mineral Mag 43: 797–807

Balog A, Read JF, Haas J (1999) Climate-controlled early dolomite, late Triassic cyclic platform carbonates, Hungary. J Sediment Res 69: 267–282

Bence AE, Albee AL (1968) Empirical correction factors for the electron microanalysis of silicates and oxides. J Geol 76: 382–403

Bodnar RJ (1992) Revised equation and table for determining the freezing point depression of H_2O–NaCl solutions. Geochim Cosmochim Acta 57: 638–684

Bodnar RJ (2003a) Introduction to fluid inclusions. In: *Samson I, Anderson A, Marshall D* (eds) Fluid Inclusions: Analysis and Interpretation, Mineral Assoc Canada, Short Course 32, Ottawa, pp 1–8

Bodnar RJ (2003b) Reequilibration of fluid inclusions. In: *Samson I, Anderson A, Marshall D* (eds) Fluid Inclusions: Analysis and Interpretation, Mineral Assoc Canada, Short Course 32, Ottawa, pp 213–230

Boettcher AL, Robertson JK, Wyllie PJ (1980) Studies in synthetic carbonatite systems; solidus relationships for $CaO–MgO–CO_2–H_2O$ to 40 kbar and $CaO–MgO–SiO_2–CO_2–H_2O$ to 10 kbar. J Geophys Res 85: 6937–6943

Cooper AF (1979) Petrology of ocellar lamprophyres from western Otago, New Zealand. J Petrol 20: 139–163

Demény A, Fórizs I, Molnár F (1994) Stable isotope and chemical compositions of carbonate ocelli and veins in Mesozoic lamprophyres of Hungary. Eur J Mineral 6: 679–690

Dunkl I (1991) Application of fission track methods in geochronological methods (in Hungarian). Ph.D. Thesis, Technical University of Miskolc, Miskolc, p 178

Embey-Isztin A, Dobosi G, Noske-Fazekas G, Árva-Sós E (1989) Petrology of a new basalt occurrence in Hungary. Mineral Petrol 40: 183–196

Esperanca S, Holloway JR (1987) On the origin of some mica-lamprophyres; experimental evidence from a mafic minette. Contrib Mineral Petrol 95: 207–216

Ferguson J, Currie KL (1971) Evidence of liquid immiscibility in alkaline ultrabasic dikes at Callender Bay, Ontario. J Petrol 12: 561–585

Fisler DK, Cygan RT (1999) Diffusion of Ca and Mg in calcite. Am Mineral 84: 1392–1399

Foley SF (1984) Liquid immiscibility and melt segregation in alkaline lamprophyres from Labrador. Lithos 17: 17–137

Goldstein RH (2003) Petrographic analysis of fluid inclusions. In: *Samson I, Anderson A, Marshall D* (eds) Fluid Inclusions: Analysis and Interpretation. Mineral Assoc Canada, Short Course 32, Ottawa, pp 9–55

Goldstein RH, Reynolds TJ (1994) Systematics of fluid inclusions in diagenetic minerals. Society for Sedimentary Geology, Short Course 31, Ottawa, p 199

Hamilton DL (1961) Nephelines as crystallization temperature indicators. J Geol 69: 321–329

Hamilton DL, MacKenzie WS (1960) Nepheline solid solution in the system $NaAlSiO_4–KalSiO_4–SiO_2–H_2O$. J Petrol 1: 56–72

Hamilton DL, Freenstone IC, Dawson JB, Donaldson CH (1979) Origin of carbonatites by liquid immiscibility. Nature 279: 52–54

Horváth I, Ódor L (1984) Alkaline ultrabasic rocks and associated silicocarbonatites in the NE part of the Transdanubian Mts. (Hungary). Mineral Slov 16: 115–119

Horváth I, Daridáné TM, Ódor L (1983) Magnesite bearing dolomitic carbonatite dike rocks from the Velence Mountains (in Hungarian). Magy Áll Földt Int Évi Jel 1981-ről, 41–44

Joesten R (1977) Mineralogical and chemical evolution of contaminated igneous rocks at a gabbro-limestone contact, Christmas Mountains, Big Bend region, Texas. Geol Soc Am Bull 88: 1515–1529

Joesten R, Hill J, Van-Horn SR (1994) Limestone assimilation and clinopyroxene production along the contacts of a 9 meter alkali olivine basalt dike. Geol Soc Am, Abstracts with Programs, 26, Killala Bay, Ireland, p 476

Kázmér M, Szabó C (1989) Late Cretaceous lamprophyre dikes in the hinterland of the Alpine deformation front. EUG-V, Terra abstract, 4, Strasbourg, p 177

Kubovics I, Szabó C (1988) Geochemical, petrologic and mineralogical study on alkali mafic and ultramafic dike rocks from Alcsutdoboz-2 drill hole (in Hungarian). Magy Áll Földt Int Évk LXV: 335–356

Kubovics I, Gál-Sólymos K, Szabó C (1985) Petrology and geochemistry of ultramafic xenoliths in mafic rocks of Hungary and Burgenland (Austria). Geol Carpathica 36: 433–450

Kubovics I, Szabó C, Gál-Sólymos K (1989) A new occurrence of lamprophyre in the Buda Mountains, Hungary. Acta Geol Hung 32: 149–168

Kubovics I, Szabó C, Harangi Sz, Józsa S (1990) Petrology and petrochemistry of Mesozoic magmatic suites in Hungary and the adjacent areas – an overview. Acta Geodaet Geophys Mont Hung 25: 345–371

Montel JM, Weisbrod A (1986) Characteristics and evolution of ''vaugneritic magmas''; an analytical and experimental approach, on the example of the Cevennes Medianes (French Massif Central). Bull Mineral 109: 575–587

Nédli Z, M. Tóth T (2003) Petrography and mineral chemistry of rhönite in ocelli of alkali basalt from Villány Mts., SW-Hungary. Acta Mineral-Petrogr 44: 51–56

Nemec D (1977) Differentiation of lamprophyre magma. Krystalinikum 13: 73–87

Owens BE (2000) High-temperature contact metamorphism of calc-silicate xenoliths in the Kiglapait Intrusion, Labrador. Am Mineral 85: 1595–1605

Phillips WJ (1973) Interpretation of crystalline spheroidal structures in igneous rocks. Lithos 6: 235–244

Philpotts AR (1990) Principles of Igneous and Metamorphic Petrology. Prentice Hall. Englewood Cliffs, New Jersey, p 498

Philpotts AR, Hodgson CJ (1968) Role of liquid immiscibility in alkaline rock genesis. XXIII. Int Geol Congr 2, pp 175–188

Rock NMS (1991) Lamprophyres. Blackie and Son, Glasgow/London/New York, p 285

Szabó C (1985) Xenoliths from Cretaceous lamprophyre of Alcsútdoboz-2. borehole, Transdanubian Central Mountains, Hungary. Acta Mineral-Petrogr 27: 39–50

Szabó C, Kubovics I, Molnár Z (1993) Alkaline lamprophyre and related dike rocks in NE Transdanubia, Hungary: The Alcsutdoboz-2 (AD-2) borehole. Mineral Petrol 47: 127–148

Vichi G, Stoppa F, Wall F (2005) The carbonate fraction in carbonatitic Italian lamprophyres. Lithos 85: 154–170

Authors' addresses: T. Azbej* (e-mail: tazbej@vt.edu) and Csaba Szabó (corresponding author; e-mail: cszabo@cerberus.elte.hu), Lithosphere Fluid Research Laboratory, Department of Petrology and Geochemistry, Eötvös University, H-1117 Budapest, Pázmány Péter sétány 1/c, Hungary; Robert J. Bodnar (e-mail: rjb@vt.edu), Fluids Research Laboratory, Department of Geosciences, Virginia Polytechnic Institute and State University, 4044 Derring Hall, VA 24061, Blacksburg, USA; Gábor Dobosi (e-mail: dobosi@geochem.hu), Institute for Geochemical Research, Hungarian Academy of Sciences, H-1112 Budapest, Budaörsi út 45, Hungary; *Fluids Research Laboratory, Department of Geosciences, Virginia Polytechnic Institute and State University, 4044 Derring Hall, VA 24061, Blacksburg, USA